Estimation of the Effective Collective Thomson Scattering Volume Using a Gaussian Beam in the LHD ECRH System

Shin KUBO, Masaki NISHIURA, Namiko TAMURA[1)], Kenji TANAKA, Takashi SHIMOZUMA, Yoshinori TATEMATSU[2)], Teruo SAITO[2)], Yasuo YOSHIMURA, Hiroe IGAMI, Hiromi TAKAHASHI, Ryosuke IKEDA[2)] and Takashi MUTOH

National Institute for Fusion Science,322-6 Oroshi-cho, Toki 509-5292, Japan
[1)]*Department of Energy Science and Technology, Nagoya University, Nagoya 464-8463, Japan*
[2)]*Research Center for Development of Far-Infrared Region, University of Fukui, Fukui 910-8507, Japan*

(Received 6 January 2009 / Accepted 2 March 2010)

Collective Thomson scattering (CTS) is a promising candidate for direct measurement of the velocity distribution function of ions in fusion devices. The relevant frequency for a CTS probing beam source is in the millimeter- to submillimeter-wave range. The scattering volume of CTS is an important parameter for determining the intensity of the scattered power and the spatial resolution of the measurement. The conventional method of estimating the scattering volume is to simply calculate the geometrical volume of the probing and receiving beams. This calculation is valid only when the beams are diffraction free. The effective scattering volume is defined and applied to a CTS system using strongly focused beams and its validity is examined experimentally.

Keywords: collective Thomson scattering, ECRH, gyrotron, Gaussian beam, scattering volume

DOI: 10.1585/pfr.5.S2103

1. Introduction

Measuring the ion velocity distribution is especially important in reactor-relevant plasmas. Collective Thomson scattering (CTS) is one of the most promising methods for evaluating the ion velocity distribution function. Despite its potential, this method has long suffered from a lack of adequate power sources. Recent developments in the high power, high frequency range of gyrotrons and in transmission techniques for electron cyclotron resonance heating (ECRH) have enabled the measurement of not only the bulk but also the high-energy component of the ion velocity distribution function [1–3].

A trial CTS measurement using the 1 MW, 77 GHz gyrotron in the Large Helical Device (LHD) has begun. Antenna sets that can generate two Gaussian beams are installed in four LHD ports. One is used to inject the probing beam and receive the scattered power. An eight channel radiometer-type receiver is set upstream of one of the transmission lines connected to the receiving antenna. Promising scattering signals are observed, well separated from electron cyclotron emission (ECE) background radiation [4]. The receiver system has been upgraded to have 32 channels and to be more sensitive in each channel.

One of the main advantages of using an ECRH system for CTS is the availability of well-defined Gaussian beams for both probing and receiving. The effective scattering cross section and its extent over the effective minor radius are the keys to determining the intensity and spatial resolution of the scattering spectra. The steering capability of the probing and receiving beams enables detailed comparison between experiment and calculation for system calibration and optimization of the scattering configuration. We describe the methods of estimating the effective scattering cross section and compare the results with those of beam steering experiments.

The methods of calculating the geometrical and effective scattering volume are described in Section 2, and the two volumes are compared in Section 3, with the Gaussian beams used for CTS in the LHD as an example. The consistency of the effective scattering volume with the measured CTS intensity during a volume scaning experiment is shown in Section 4. The conclusion is given in Section 5.

2. Scattering Volume

The scattering volume defined in scattering measurements is generally the purely geometrical cross section of the probing and receiving beams. Assuming uniformity of the scattering characteristics, beam, and sensitivity profile in a unit volume, the scattered power density P_s at the far field $\boldsymbol{R}$ in a unit angle frequency in a unit steradian can be expressed as

$$P_s(\boldsymbol{R},\omega_s)\mathrm{d}\Omega\mathrm{d}\omega_s = \int_V p_i(\boldsymbol{r})\frac{r_0^2}{2\pi}\left|\hat{\boldsymbol{s}}\times\hat{\boldsymbol{s}}\times\hat{\boldsymbol{E}}_i\right|^2 n_e(\boldsymbol{r})\,S(\boldsymbol{K},\omega)\,\mathrm{d}\boldsymbol{r}. \quad (1)$$

$\hat{\boldsymbol{E}}_i$ and $\hat{\boldsymbol{s}}$ are the unit vectors in the oscillating electric field direction of the probing beam and in the direction of the

author's e-mail: kubo@LHD.nifs.ac.jp

scattered wave vector $\boldsymbol{k}_\mathrm{s}$, respectively. $\boldsymbol{k}_\mathrm{i}$ and $\boldsymbol{K}$ are the wave vectors of the probing beam and the fluctuations that causes scattering, respectively. ω_i, ω, and ω_s are the angular frequencies of the probing beam, fluctuation, and scattered radiation, respectively. The relations $\boldsymbol{k}_\mathrm{s} = \boldsymbol{k}_\mathrm{i} + \boldsymbol{K}$ and $\omega_\mathrm{s} = \omega_\mathrm{i} + \omega$ are satisfied. r_0 is the classical electron radius. $p_\mathrm{i}(\boldsymbol{r})$ is the power density of the incident beam. $n_\mathrm{e}(\boldsymbol{r})$ and $S(\boldsymbol{K}, \omega)$ are the local electron density and a form factor that depends on local plasma parameters, respectively. This equation should be integrated over all the space where scattering can occur. When the plasma parameters n_e, $S(\boldsymbol{K}, \omega)$ and $|\hat{\boldsymbol{s}}\times\hat{\boldsymbol{s}}\times\hat{\boldsymbol{E}}|^2$ are constant over the volume, Eq. (1) can be simplified to yield the conventional formula [5] for the total receiving power P_r with the antenna efficiency function $\eta_r(\boldsymbol{r})$ as

$$P_\mathrm{r} = \int p_\mathrm{i}(\boldsymbol{r})\eta_\mathrm{r}(\boldsymbol{r})\frac{r_0^2}{2\pi}\left|\hat{\boldsymbol{s}}\times\hat{\boldsymbol{s}}\times\hat{\boldsymbol{E}}\right|^2 n_e(\boldsymbol{r})S(\boldsymbol{K},\omega)\,\mathrm{d}\boldsymbol{r} = \frac{r_0^2}{2\pi}\frac{P_\mathrm{i}}{A}V\left|\hat{\boldsymbol{s}}\times\hat{\boldsymbol{s}}\times\hat{\boldsymbol{E}}\right|^2 \overline{n_\mathrm{e}}\,\overline{S(\boldsymbol{K},\omega)}, \quad (2)$$

where $\overline{n_\mathrm{e}}$ and $\overline{S(\boldsymbol{K},\omega)}$ are the average electron density and the form factor of the scattering volume, respectively. V and A are the scattering volume and the crosssection of the probing beam, respectively. These values can be calculated independently using the geometrical overlap between the probing and receiving beams and the cross section of the probing beam when the changes in the spot sizes of both beams near the scattering center are negligible. The precise combined expression for A and V can be derived from Eq. (2) as the integral

$$\frac{P_\mathrm{i}}{A}V = \iint p_\mathrm{i}(\boldsymbol{r})\eta_\mathrm{r}(\boldsymbol{r}')\times\delta(\boldsymbol{r}' - \overleftrightarrow{\boldsymbol{T}}\cdot\boldsymbol{r})\mathrm{d}\boldsymbol{r}\mathrm{d}\boldsymbol{r}'. \quad (3)$$

The power density distribution function $p_\mathrm{i}(\boldsymbol{r})$ is

$$p_\mathrm{i}(\boldsymbol{r}) = \frac{2P_\mathrm{i}}{\pi w_x(z)w_y(z)}\exp\left[-2\left(\frac{x^2}{w_x^2(z)} + \frac{y^2}{w_y^2(z)}\right)\right], \quad (4)$$

and the antenna efficiency function, $\eta_\mathrm{r}(\boldsymbol{r}')$ is

$$\eta_\mathrm{r}(\boldsymbol{r}') = \frac{w_{x'}(z'_\mathrm{c})w_{y'}(z'_\mathrm{c})}{w_{x'}(z')w_{y'}(z')}\exp\left[-2\left(\frac{x'^2}{w_{x'}^2(z')} + \frac{y'^2}{w_{y'}^2(z')}\right)\right]. \quad (5)$$

Two elliptic Gaussian beams are defined by their e-folding waist sizes of the oscillating electric field, $w_{0,\sigma}$, $w'_{0,\sigma'}$, and waist positions $z_{0,\sigma}$, $z'_{0,\sigma'}$, expressed in the coordinate system (x, y, z) for the probing beam and (x', y', z') for the receiving beam as

$$w_\sigma^2(z) \equiv w_{0,\sigma}^2 + \frac{\lambda^2(z - z_{0,\sigma})^2}{\pi^2 w_{0,\sigma}^2}, \sigma = x \text{ or } y,$$
$$w_{\sigma'}^2(z') \equiv w_{0,\sigma'}^2 + \frac{\lambda^2(z' - z'_{0,\sigma'})^2}{\pi^2 w'^2_{0,\sigma'}}, \sigma' = x' \text{ or } y'. \quad (6)$$

λ is the wavelength of the radiation under consideration, and z'_c is the z' value of the scattering center in the (x', y', z') coordinate system. The matrix $\overleftrightarrow{\boldsymbol{T}}$ is the transformation matrix between the coordinate systems of the probing and receiving beams, (x, y, z) and (x', y', z').

The geometrical scattering volume V_geom and the probing beam crosssection A can be defined geometrically as

$$V_\mathrm{geom} = \iint \exp\left[-2\left(\frac{x^2}{w_x^2(z)} + \frac{y^2}{w_y^2(z)}\right)\right] \times\exp\left[-2\left(\frac{x'^2}{w_{x'}^2(z')} + \frac{y'^2}{w_{y'}^2(z')}\right)\right] \times\delta(\boldsymbol{r}' - \overleftrightarrow{\boldsymbol{T}}\cdot\boldsymbol{r})\mathrm{d}\boldsymbol{r}\mathrm{d}\boldsymbol{r}', \quad (7)$$

$$A = \iint_{z=z_c} \exp\left[-2\left(\frac{x^2}{w_x^2(z)} + \frac{y^2}{w_y^2(z)}\right)\right]\mathrm{d}x\mathrm{d}y = \frac{\pi w_x(z_\mathrm{c})w_y(z_\mathrm{c})}{2}. \quad (8)$$

These values of V_geom and A can be used for the scattering volume V and A in Eq. (2) only if the changes in spot size along the beam axis are negligible over the beam overlap region. The effective scattering volume V_eff can now be defined using Eqs. (3) and (8) as

$$V_\mathrm{eff} = \iint \frac{w_x(z_\mathrm{c})w_y(z_\mathrm{c})}{w_x(z)w_y(z)}\exp\left[-2\left(\frac{x^2}{w_x^2(z)} + \frac{y^2}{w_y^2(z)}\right)\right] \times\eta_\mathrm{r}(\boldsymbol{r}')\delta(\boldsymbol{r}' - \overleftrightarrow{\boldsymbol{T}}\cdot\boldsymbol{r})\mathrm{d}\boldsymbol{r}\mathrm{d}\boldsymbol{r}'. \quad (9)$$

Note that the formulas derived above are not applicable when the refraction effect is so large that the beam cannot propagate as a Gaussian beam.

3. Comparison of the Geometrical and Effective Scattering Volumes

In the LHD's CTS system, the probing and receiving beams are defined by the ECRH antenna system, which uses strongly focused Gaussian optics. The designed beam profiles are shown in Figs. 1 (a) and (b). Both beams are depicted as tubes representing elliptical spot sizes along the beam axes. An advantage of using the ECRH antenna system as a CTS system is that the probing and receiving beams are well documented [6]. When strongly focused beams are used, as in the LHD scattering configuration, the power density and antenna efficiency change along the optical axis. In such cases, the deviation of V_eff from V_geom becomes large. Figure 1 shows two cases in which the probing and receiving beams cross (a) at the midplane of LHD and (b) at 0.5 m above the midplane. The beams cross near the waist points of each beam in (a), but farther from the waist points in (b). To see in greater detail the difference between V_geom as defined in Eq. (7) and V_eff as defined in Eq. (9), a three-dimensional plot of the calculated points is shown in Figs. 1 (c)-(f). Points are plotted three dimensionally with different shapes and colors representing several levels of the integrands of Eqs. (7) and (9) for the conditions in Figs. 1 (a) and (b). Figs. 1 (c) and (e) are plots of

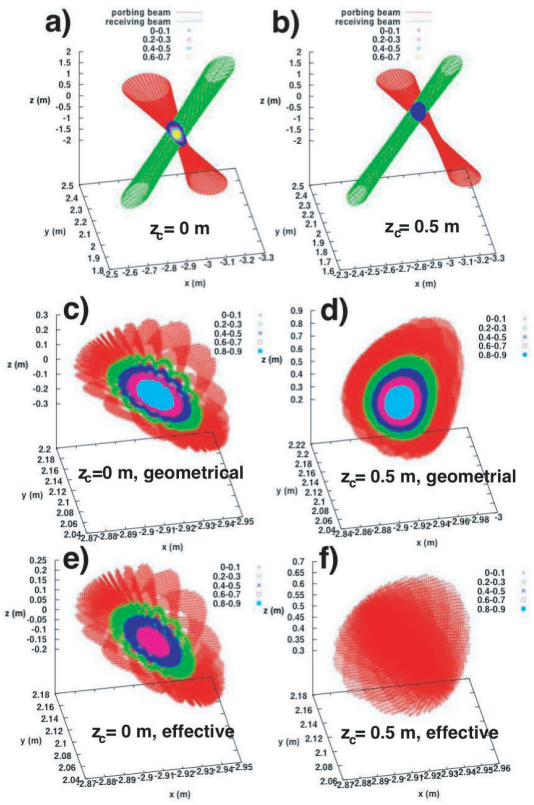

Fig. 1 Configuration of the probing and receiving beams in the LHD when the scattering center is located on (a) the midplane ($z = 0$ m) and (b) $z = 0.5$ m. Profiles of the integrand of $V_{\rm eff}$ as defined in Eq. (9) are also plotted. Detailed profiles of the integrand are shown in (c)-(f). (c) and (d) show profiles of the integrands of $V_{\rm geom}$ as defined in Eq. (7). (e) and (f) show those of $V_{\rm eff}$ as defined in Eq. (9). In (c) and (e) the scattering center is at $z = 0$ m, and in (d) and (f) at $z = 0.5$ m. All calculated points belonging to the levels 0-0.1, 0.2-0.3, 0.4-0.5, 0.6-0.7, and 0.8-0.9 are plotted with red pluses, green crosses, blue stars, magenta squares and cyan closed squares, respectively.

$V_{\rm geom}$ and $V_{\rm eff}$, respectively, for beams crossing at the midplane [corresponding to Fig. 1 (a)]. Figs. 1 (d) and (f) are those for the beams crossing at 0.5 m above the midplane [Fig. 1 (b)]. The beam expansion effects are clear in both the probing beam intensity and the receiving efficiency especially when the beams cross away from the waist position.

Figure 2 shows the dependence of the calculated $V_{\rm geom}$ and $V_{\rm eff}$ on the radial position of the scattering center. In this case, $V_{\rm geom}$ and $V_{\rm eff}$ coincide within 20%, since the waist position of the probing and receiving beams stay near the scattering center within the antenna's steerable range (3.4-3.8 m). An advantage to calculating the scattering volume using the integral form, as in Eq. (7) or (9), is that the spatial resolution of the scattering measurement can be defined as the standard deviations of the plasma parameters away from the scattering center. Figures 3 (a) and (b) show the dependence of the average minor radius ρ and magnetic

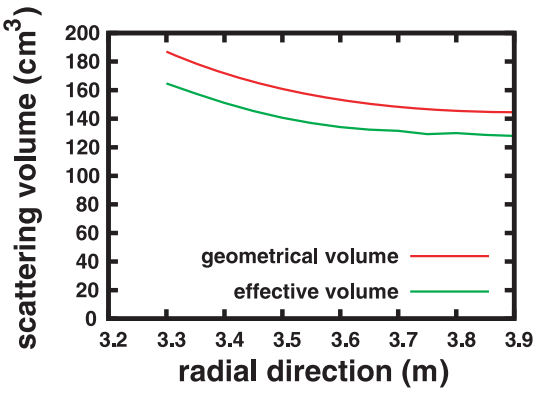

Fig. 2 Dependence of $V_{\rm geom}$ and $V_{\rm eff}$ on radial direction.

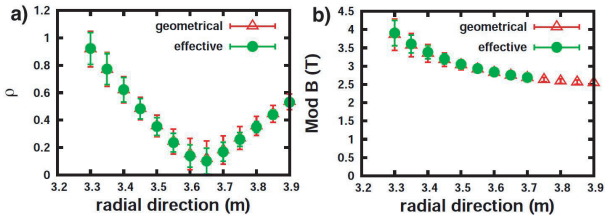

Fig. 3 Dependence of the (a) ρ and (b) B and their standard deviations on $V_{\rm geom}$ and $V_{\rm eff}$ during a radial scan of the volume center.

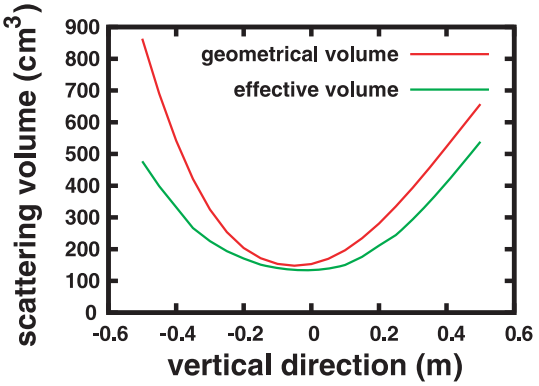

Fig. 4 Variation in $V_{\rm geom}$ and $V_{\rm eff}$ during a vertical scan of the volume center.

field strength with their standard deviations on the scattering volume. These results show that a radial scan of the scattering center give a good measure of the radial distribution of the ion velocity distribution function within the resolution of $\delta\rho \approx 0.1$.

In contrast, vertical scans of the scattering center are severely affected by the expansion of the probing and receiving beams. Figure 4 shows the depenence of $V_{\rm geom}$ and $V_{\rm eff}$ on the vertical position of the scattering center. The deviation of $V_{\rm geom}$ from $V_{\rm eff}$ becomes large as the scattering center moves away from the waist positions of the probing and receiving beams. The spatial resolution and extent of the magnetic field also widen (see Fig. 5).

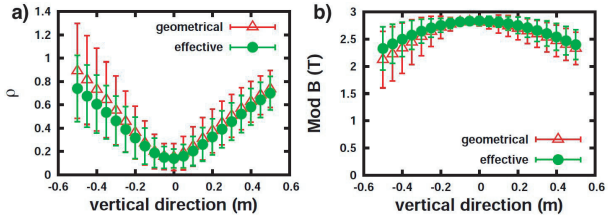

Fig. 5 Dependence of the (a) ρ and (b) B with their standard deviation on the geometrical and effective scattering volume during the vertical scan of the volume center.

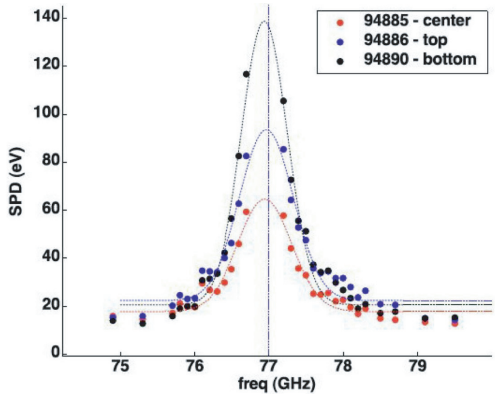

Fig. 6 Scattered power spectrum from NBI-heated plasma with $n_e = 1 \times 10^{19}$ m^{-3}, and $T_{e,0} = 2.2$ keV.

4. Comparison with Experimental Data

A scattering volume scan experiment was performed using a 32-channel receiver system. The scattered power spectra for a scattering center scan in the vertical direction are shown in Fig. 6. The target plasmas were reproducible and were sustained by NBI with an electron density $n_e = 1 \times 10^{19}$ m^{-3} and electron temperature at the center, $T_{e,0} = 2.2$ keV. The density profile is broad and is almost the same at $z = 0, \pm 0.5$ m. A ray tracing calculation under this experimental condition indicates that the beam propagates as a Gaussian beam and the deviation from that in the vacuum is negligible. The ion temperature estimated from the Doppler broadening of the Ar line was about 1 keV. The relative sensitivity of each channel was calibrated using the difference between the black-body radiation intensity of liquid N_2 and room temperature. The background ECE intensities were at the level of 20 eV in these cases. After subtracting the background, the spectral intensity ratio for the bottom, center, and top cases were 2.9:1.0:1.8. As Eq. (2) showed, the scattered spectral intensity is proportional to the volume V and inversely proportional to the probing beam cross section A. The relative spectral intensity, except for the plasma parameters, scales to the effective length, V/A. Figure 7 shows the calculated V/A with the measured intensity normalized at the center. The good agreement between the relative intensity of the scattered spectra and the effective length V/A using V_{eff} indicates that the observed spectra reflect the local ion velocity distribution function defined by the designed Gaussian beam optics.

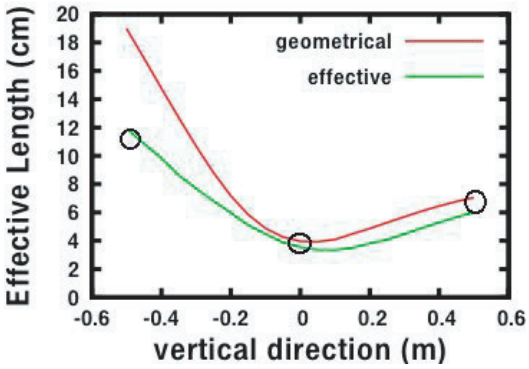

Fig. 7 V_{geom}/A and V_{eff}/A, during a vertical scan of the volume center. Open circles indicate the relative intensity of the scattered spectra normalized by that at the center.

5. Conclusion

A method of calculating the scattering volume for an elliptical Gaussian beam is established. The difference between the geometrical and effective scattering volumes becomes large for a strongly focused system, since the effect of beam expansion is not negligible. Comparing the experimental data during a vertical scattering center scan with the scattered spectrum intensity confirms the effectiveness of the scattering length defined by V/A and the adequacy of the LHD's scattering system.

Acknowledgement

The authors are grateful to Drs. S. Korsholm and F. Meo for their invaluable comments during their stay at National Institute for Fusion Science (NIFS) under the international collaboration project of the National Institutes of Natural Sciences. This work was supported by Grants-in-Aid for Scientific Research (KAKENHI 20026009 and 21360455) and also partly by the NIFS (NIFS09ULRR501 and 503).

[1] H. Bindslev, S. K. Nielsen, L. Porte, J. A. Hoekzema, S. B. Korsholm, F. Meo, P. K. Michelsen, S. Michelsen, J. W. Oosterbeek, E. L. Tsakadze, E. Westerhof and P. Woskov, Phys. Rev. Lett. **97**, 205005 (2006).
[2] F. Meo, H. Bindslev, S. B. Kolsholm, E. L. Tsakadze, C. I. Walker *et al.*, Rev. Sci. Instrum. **75**, 3585 (2004).
[3] M. Nishiura, K. Tanaka, S. Kubo, T. Saito, Y. Tatematsu *et al.*, Rev. Sci. Instrum. **79**, 10E731 (2008).
[4] S. Kubo, M. Nishiura, K. Tanaka, T. Shimozuma, Y. Tatematsu, T. Notake, T. Saito, Y. Yoshimura, H. Igami, H. Takahashi and N. Tamura, to be published in PFR (2010).
[5] J. Sheffield, "Plasma Scattering of Electro-manetic Radiation", Academic Press, New York, 1975, eq.(2.3.17).
[6] S. Kubo, T. Shimozuma, Y. Yoshimura, H. Igami, H. Takahashi *et al.*, Proc. 22nd IAEA Fusion Energy Conference, 13-18 October 2008 Geneva, Switzerland. EX/P6-14.